

Supplementary Information for

Brain-wide functional connectivity of face patch neurons during rest

Daniel Zaldivar^{1,*}, Kenji W. Koyano¹, Frank Q. Ye², David C. Godlove¹,
Soo Hyun Park¹, Brian E. Russ¹, Rebecca Bhik-Ghanie¹, David A. Leopold^{1,2,*}

¹ Section on Cognitive Neurophysiology and Imaging, National Institute of Mental Health, Bethesda, MD 20892, USA.

² Neurophysiology Imaging Facility, National Institute of Mental Health, National Institute for Neurological Disorders and Stroke, National Eye Institute, National Institute of Health, Bethesda, MD 20892, USA

*Correspondence:

Daniel Zaldivar, E-mail: daniel.zaldivarperez@nih.gov or

David Leopold, E-mail: leopoldd@mail.nih.gov

This PDF file includes:

Supplemental Figures S1-S12

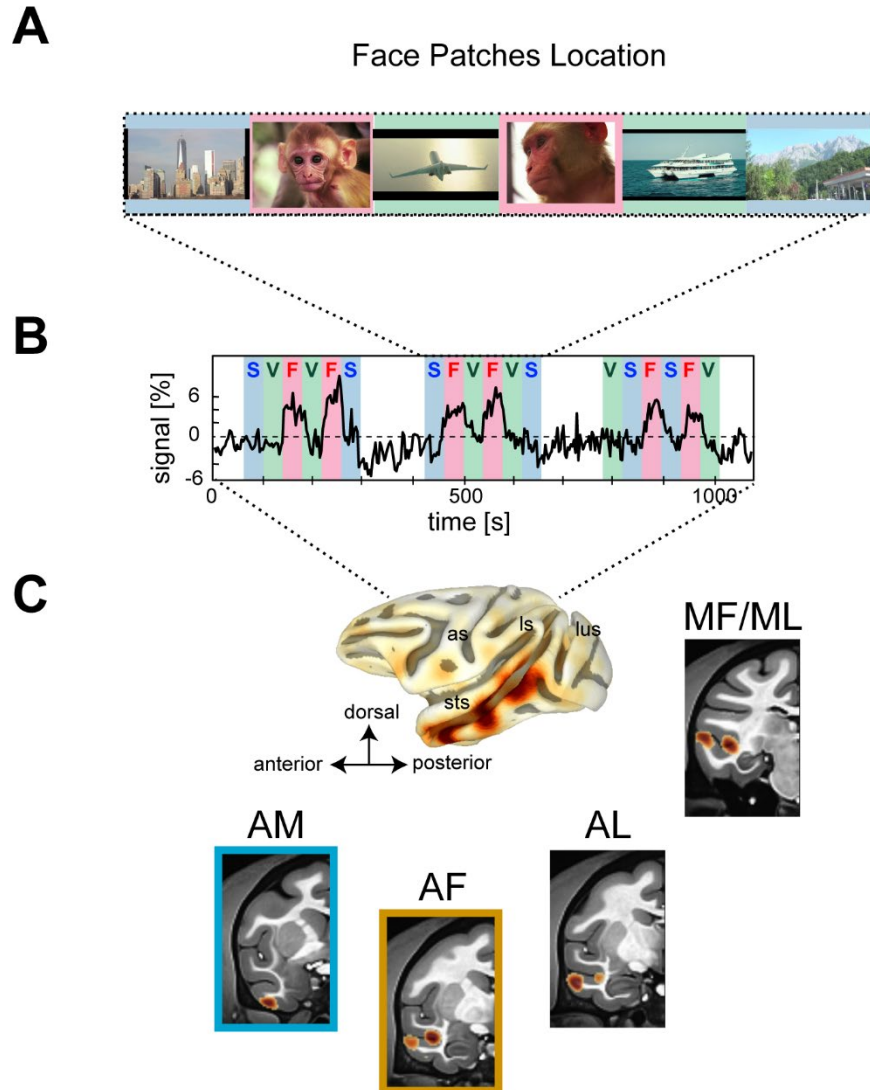


Fig. S1 fMRI targeting of face selective areas. (A) Schematic representation of the visual stimulation paradigm used for the fMRI-targeting of face patches. (B) fMRI response time series of a voxel located in the AF face patch showing selective response to the presentation of faces (shaded red area) in contrast to other objects (e.g., vehicles, shaded green area) or visual scenes (shaded blue area). (C) Cortical surface depicting the location of the face selective areas. Structural MRI and functional overlay showing activation in voxels corresponding to the face patch AM (anterior-medial), AF (anterior-fundus), AL (anterior-lateral), ML (medio-lateral) and MF (medio-fundus) face patch areas in monkey M4.

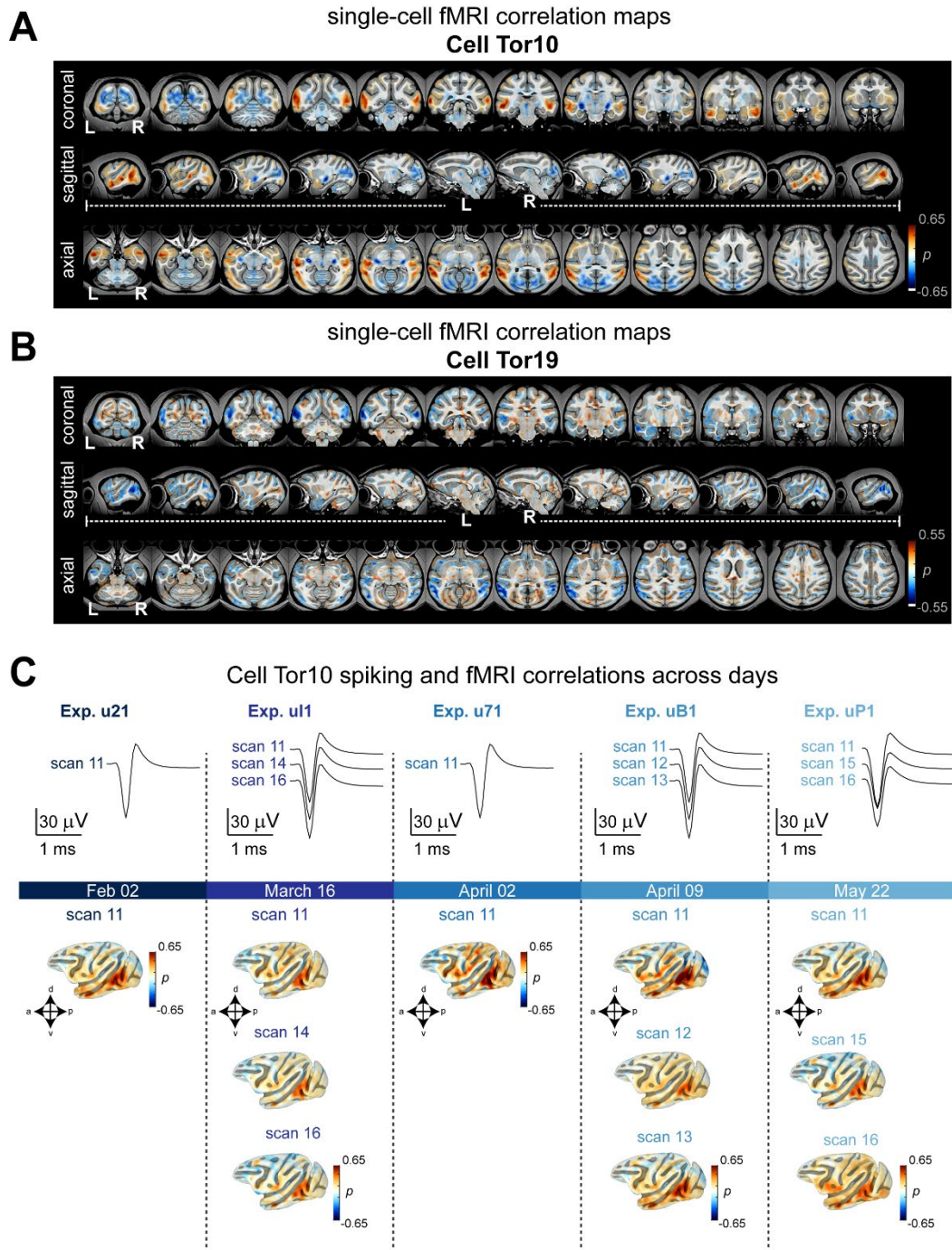


Fig. S2 Consistent single-unit fMRI maps across days. Single-unit fMRI maps from two example neurons recorded in the left AF. Activation maps for cell (A), Tor10 and (B) cell Tor19, are displayed in the coronal (top), sagittal (middle) and axial (bottom) planes. (C) Consistency of single-unit fMRI activation maps from cell Tor10 collected across different scans and during multiple days. Each column depicts: the spike wave form from cell Tor10 recorded over the course of 4 months and during different scans (top); the cortical surface representation of the fMRI response from the recording hemisphere is depicted across days and scans (bottom). Dates of simultaneous fMRI and neurophysiology recordings are indicated in the blue rectangles.

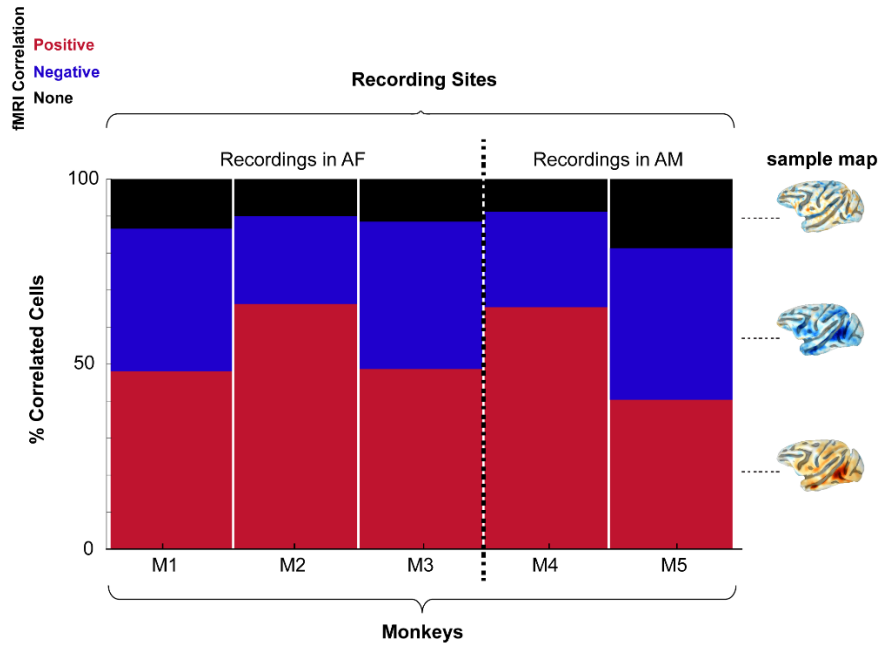


Fig. S3 Proportion of single-unit fMRI functional maps. Percentage of single-unit functional maps in each monkey with positive (red), negative (blue) and lack of correlational structure (black).

Single-Unit fMRI maps extracted from recordings in AF

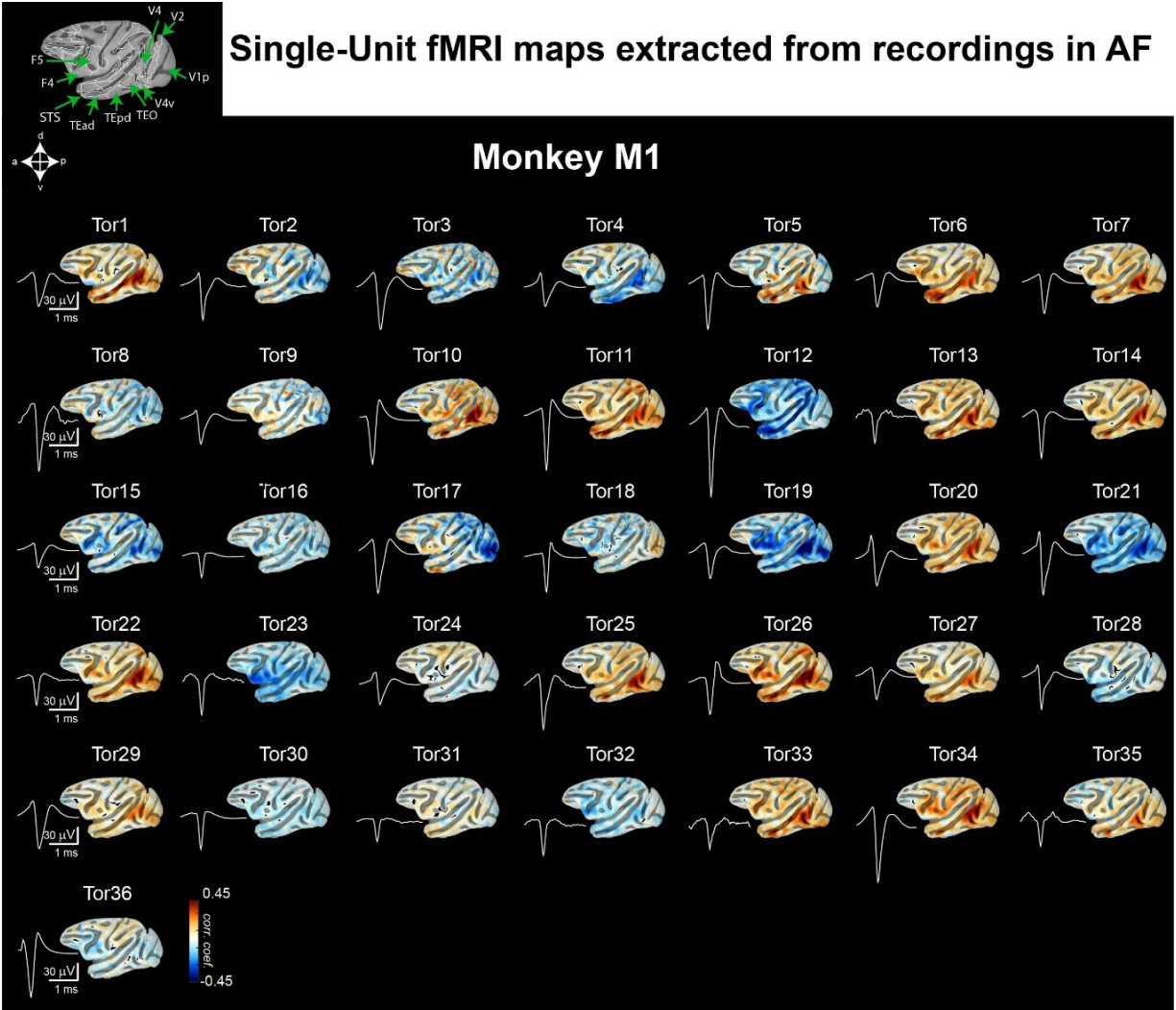


Fig. S4A Single-unit functional map from all single neurons recorded from monkey M1, accompanied by their respective spike wave form.

Single-Unit fMRI maps extracted from recordings in AF

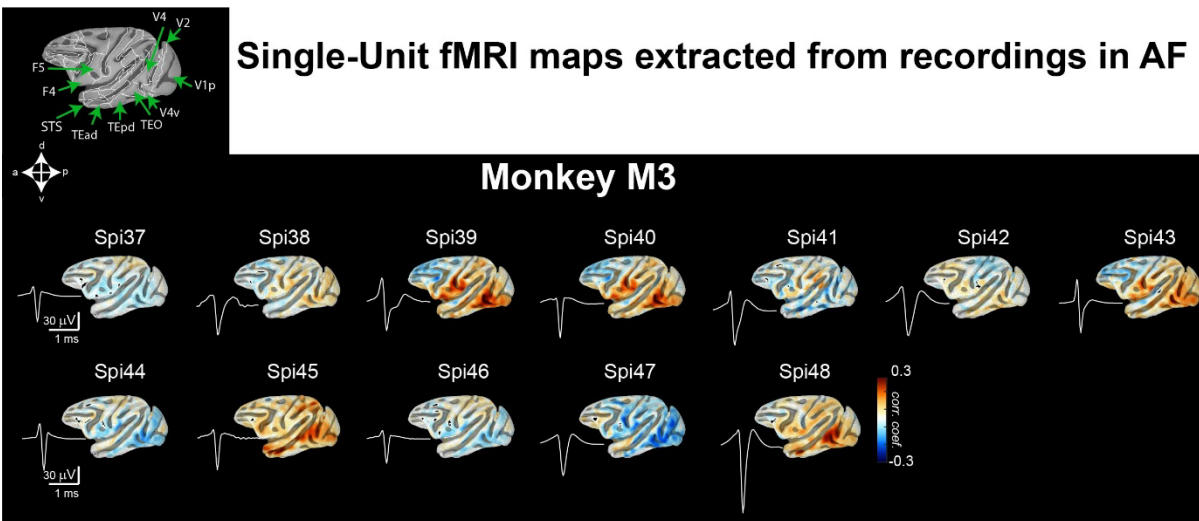


Fig. S4C Single-unit functional maps from all single neurons recorded from monkey M3, accompanied by their respective spike wave form.

Single-Unit fMRI maps extracted from recordings in AM

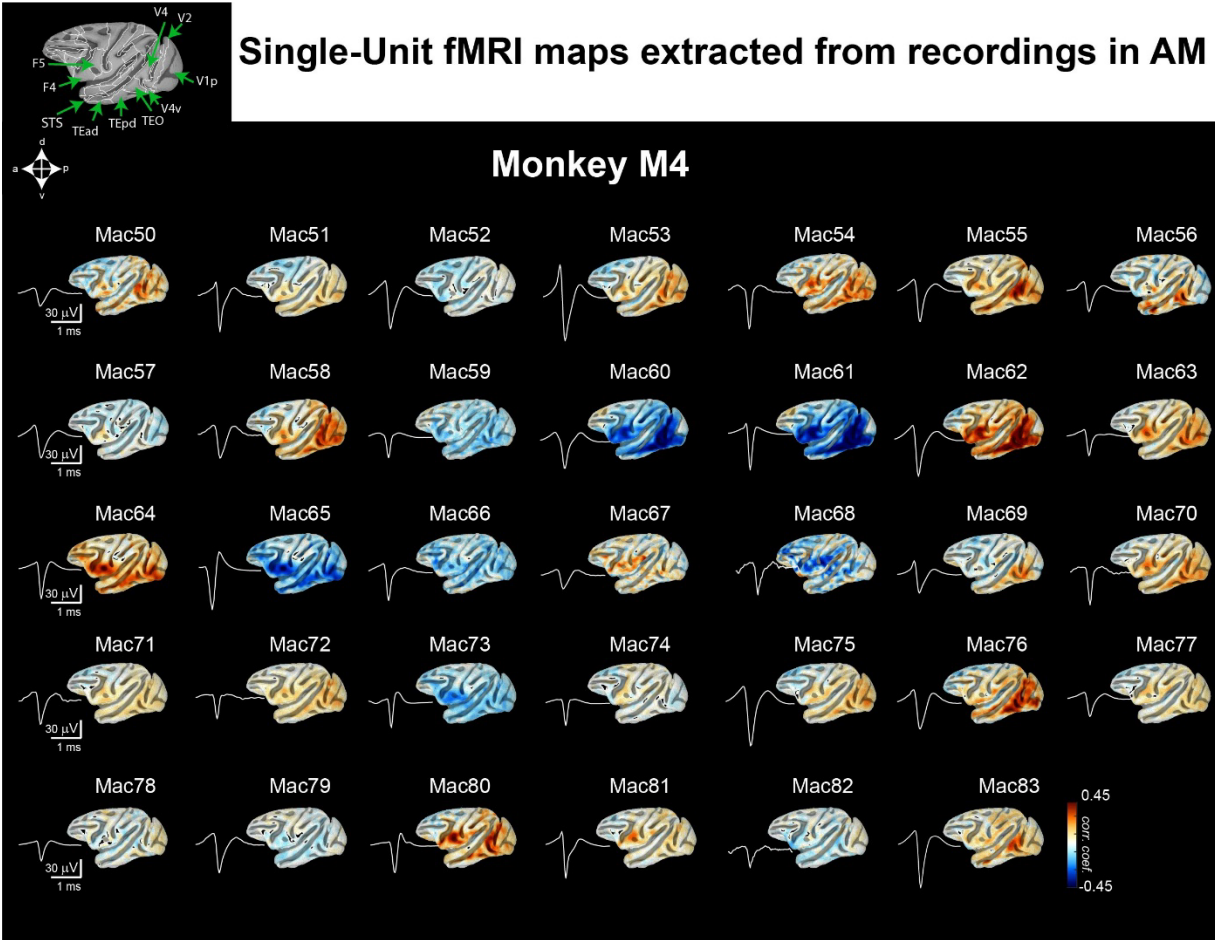


Fig. S5A Single-unit functional maps from all single neurons recorded from monkey M4, accompanied by their respective spike wave form.

Single-Unit fMRI maps extracted from recordings in AM

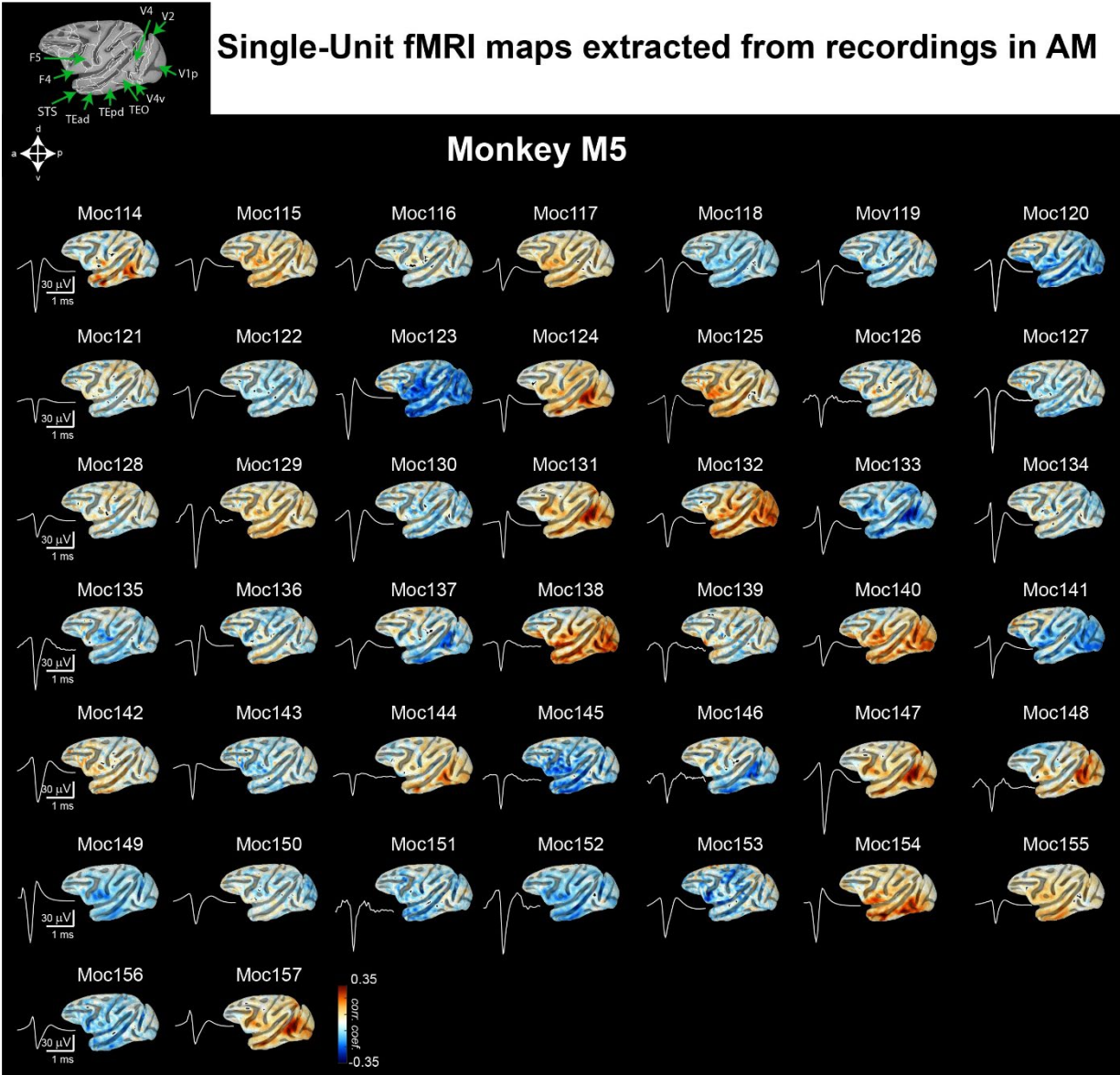


Fig. S5B Single-unit functional maps from all single neurons recorded from monkey M5, accompanied by their respective spike wave form.

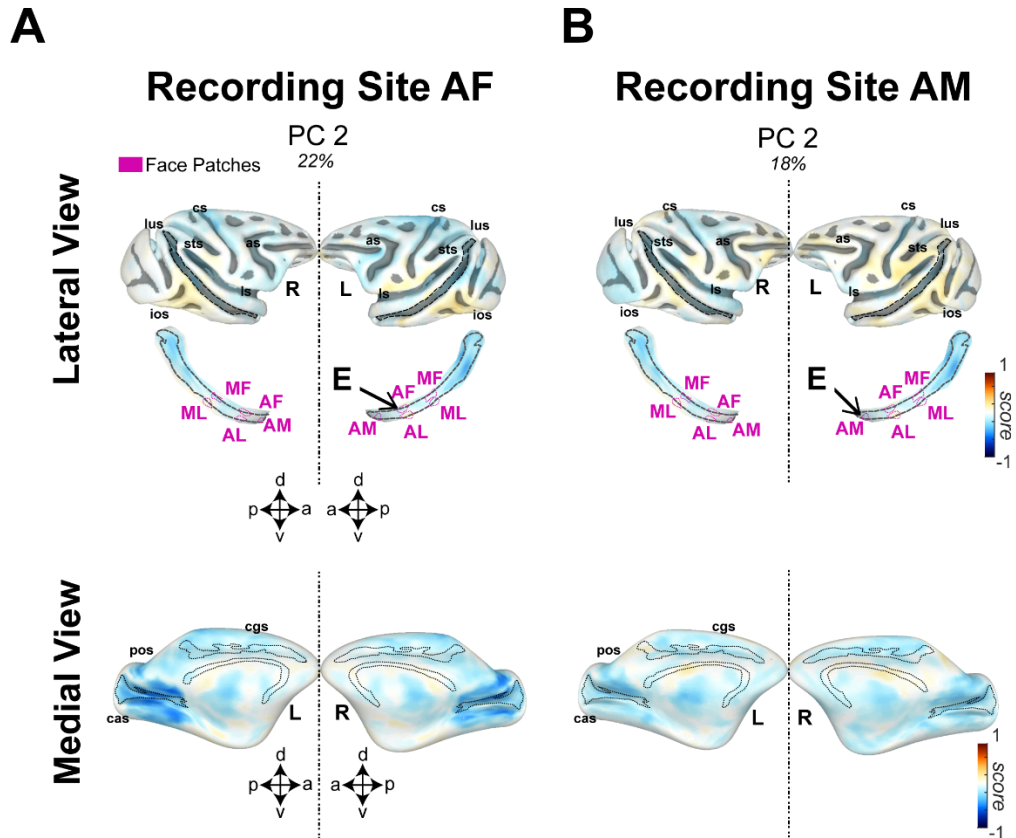


Fig. S6 Results from the second PC. Functional maps showing the results obtained from PCA analysis. Results are showing the second PC from recordings in **(A)**, AF and in **(B)**, AM. Lateral (top panel) and medial (bottom panel) views are shown for each corresponding recording site. “E” demarks the location of the electrode.

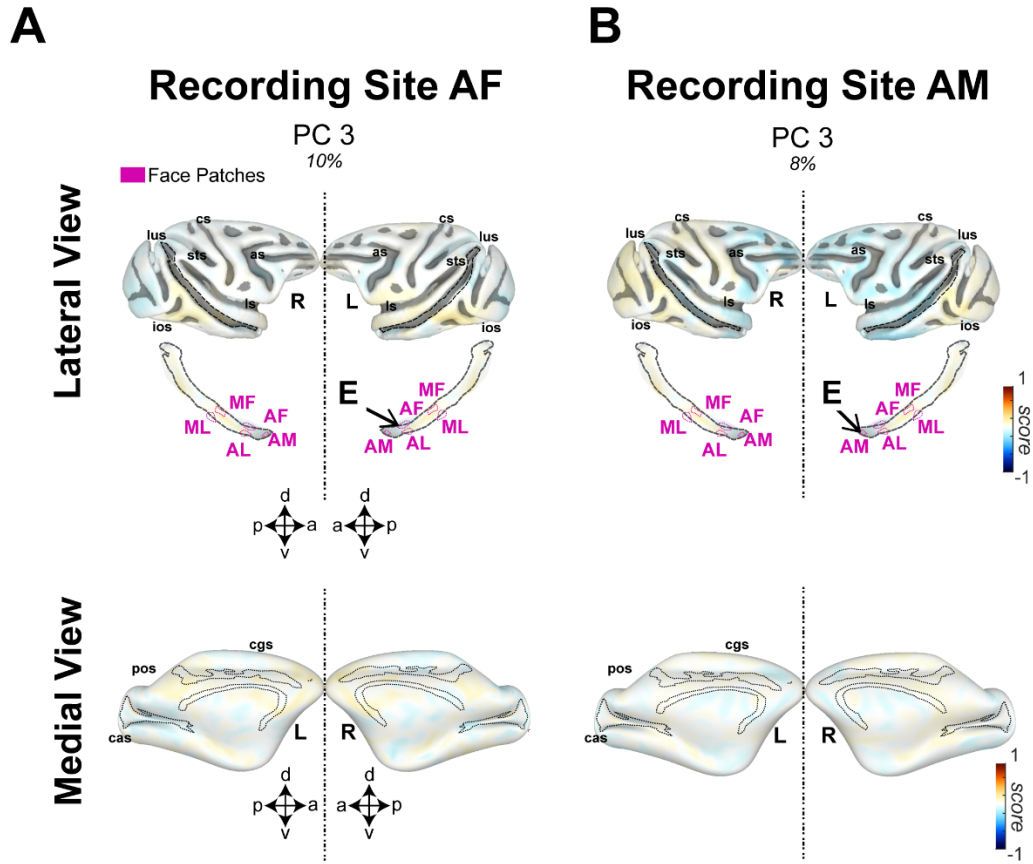


Fig. S7 Results from the third PC. Functional maps showing the results obtained from PCA analysis. Results are showing the third PC from recordings in **(A)** AF and in **(B)** AM. Lateral (top panel) and medial (bottom panel) views are shown for each corresponding recording site. “E” demarks the location of the electrode.

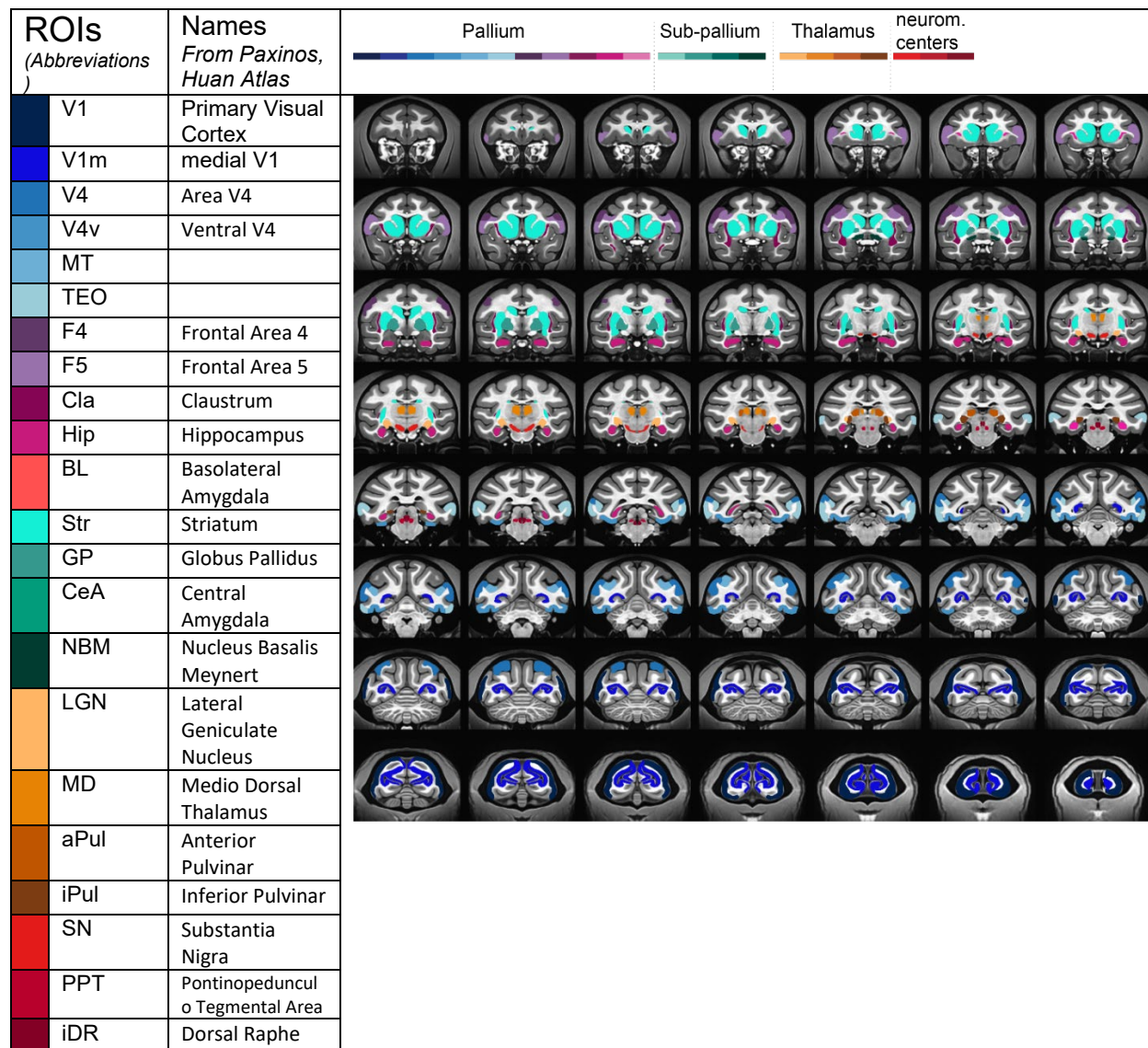


Fig. S8 Location and extent of ROIs. The color code and name list in the left indicate the ROIs' location in high-resolution MRI anatomical images. Cortical and subcortical structures are categorized according to their anatomical location relative to the subdivisions of the standard developmental brain (panel on top of anatomical images). The ROIs that we used here, as the initial template were first defined interactively using custom software on an average monkey brain.

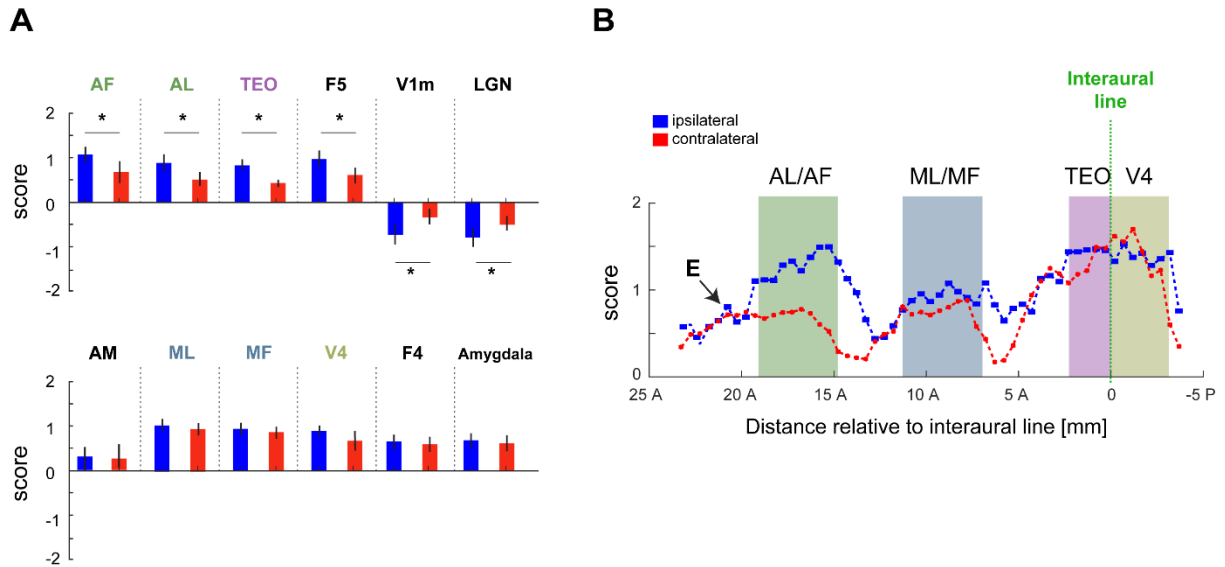


Fig. S9 Hemispheric differences in fMRI response in AM. Difference in functional activity between the recording hemisphere, or ipsilateral, and the contralateral hemisphere. **(A)** comparison between the ipsilateral (shown in blue) and the contralateral (shown in red) hemispheres from regions showing significant differences in their fMRI coupling to the spiking activity (top panel) and regions with no evident difference across the two hemispheres (bottom panel). **(B)**, distribution of the fMRI coupling to the spiking activity along the V4/IT axis. The structure and organization in this figure are the same as in **Fig. 5**.

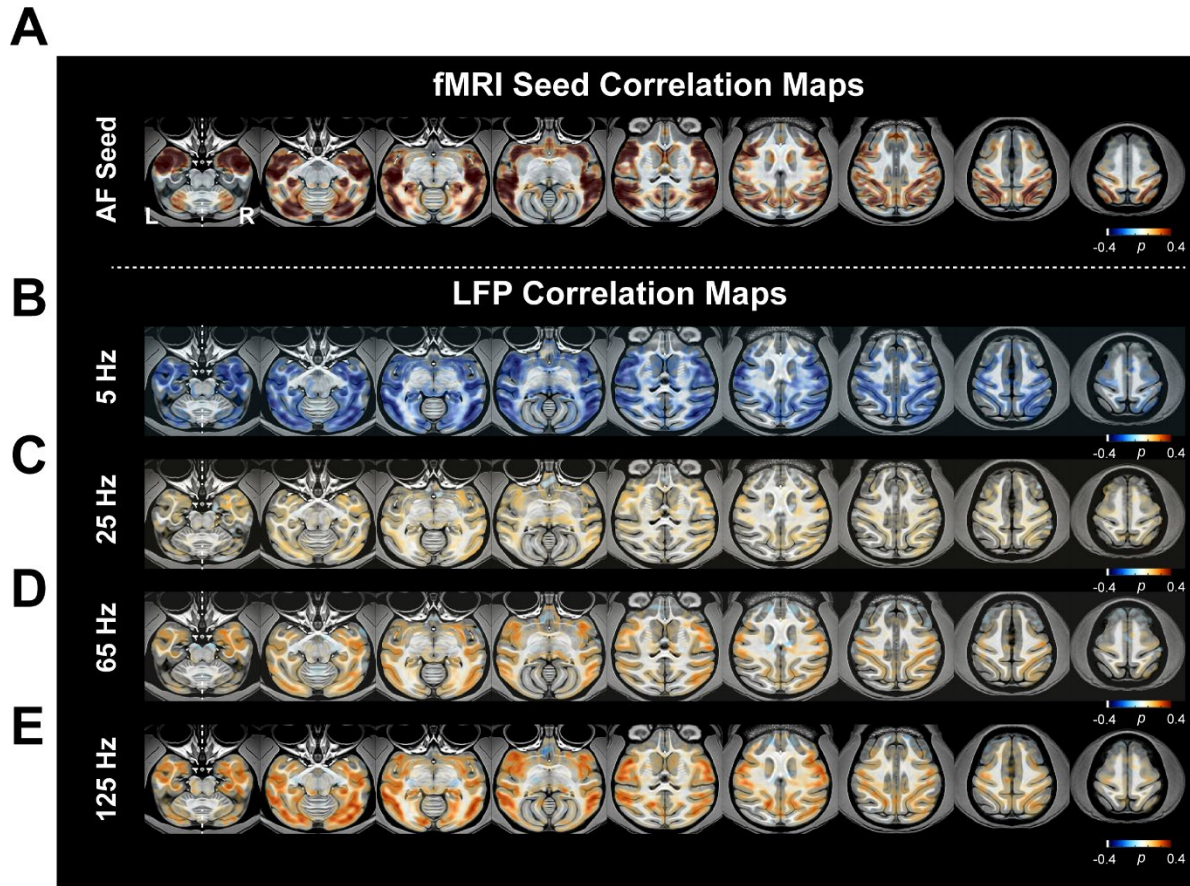


Fig. S10 Correlation maps based on the local population signals. Whole-brain functional maps extracted associated to the **(A)** fMRI seed in the AF face patch, and with selected LFPs bands: **(B)** 5 Hz; **(C)** 25 Hz; **(D)** 65 Hz; and **(E)** 125 Hz frequency ranges.

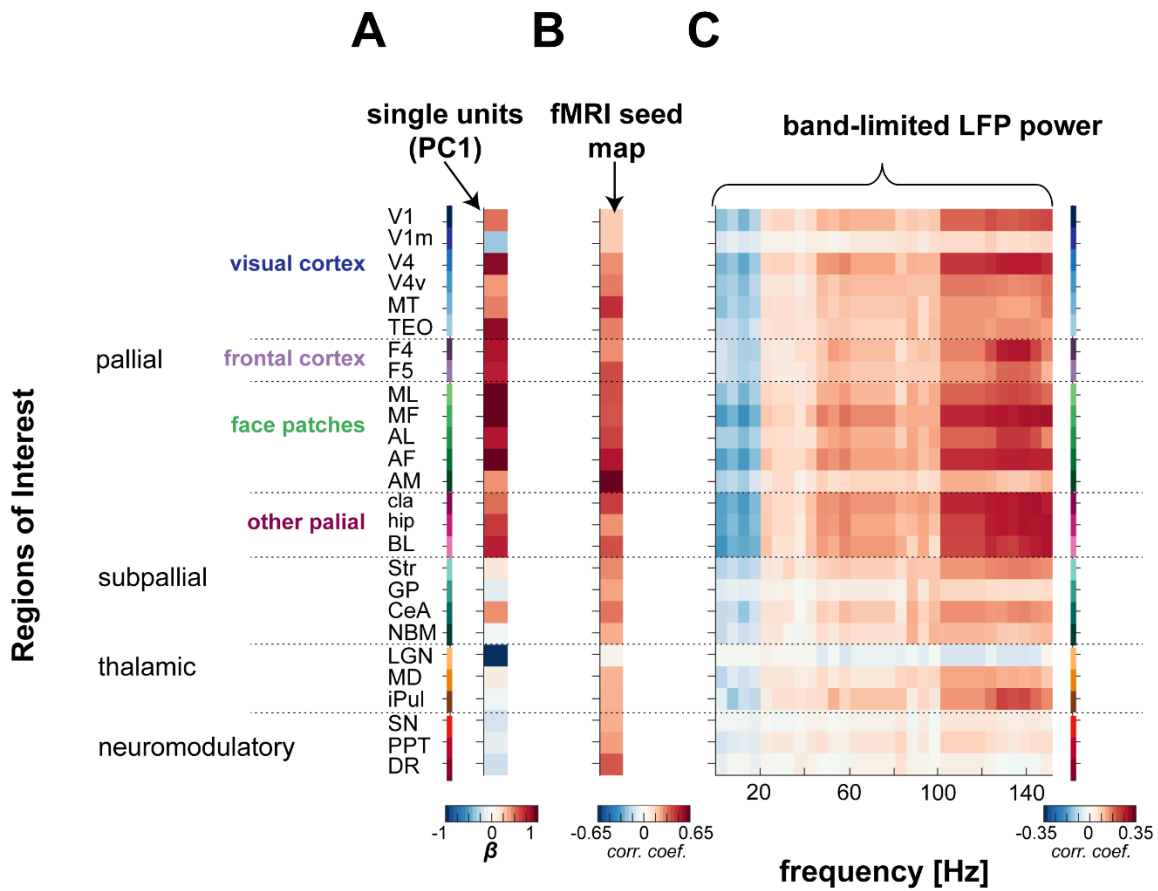


Fig. S11 Comparison of local population signals with the single-unit fMRI activity. (A) fMRI profiles from the population spiking activity in AM, (B) fMRI seed in AM (seed across $n = 20$ scans). (C) the correlation profiles across different LFP frequency bands spaced by 5 Hz each ($n = 30$ columns representing 30 LFP frequencies). The organization and structure in this figure are the same as in Fig. 6 (see also Fig. S8 for the ROIs names and their spatial extent).

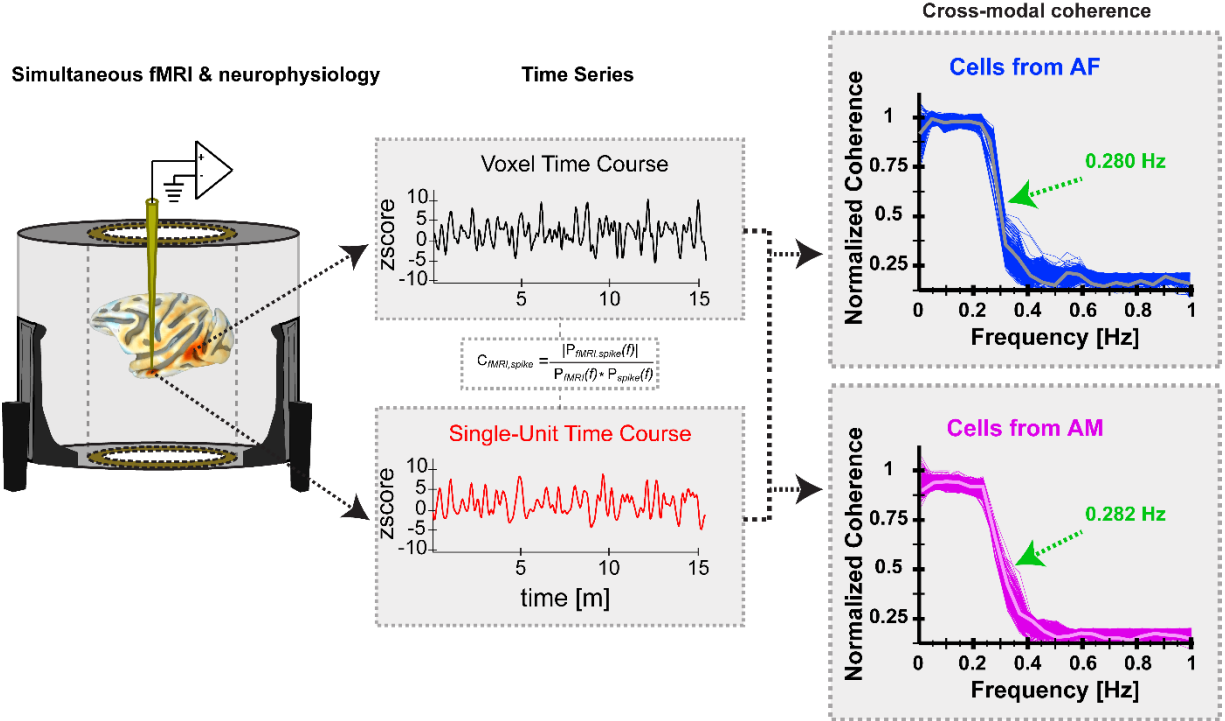


Fig. S12 Cross-modal relationship between fMRI and single unit spiking activity. We quantified the frequency correspondence between the spiking activity and fMRI voxels. Coherence estimates were computed as magnitude-squared coherence $C_{fMRI, spike}(f)$ using the Welch's average, modified periodogram method as shown in formula depicted in the figure. $P_{fMRI}(f)$ corresponds to the spectral densities from voxel's time courses in ROIs ($n= 6$, areas include face patches and V4) with high correlation values (total number of voxels = 852) and $P_{spike}(f)$ from time courses extracted from the spiking activity (in blue are 37 single units recorded from AF and in purple are 34 single units recorded from AM). The absolute coherence was normalized so that we could focus on the frequency cutoff which was estimated by taking the frequency at which coherence between the two signals dropped to half of its maximum value. For both AM and AF the cutoff was ~ 0.28 Hz (indicated by the green arrows in both AF and AM panels).